Multilevel Coded Modulation for the Full-Duplex Relay Channel

Ahmed Attia Abotabl, *Student Member, IEEE*, and Aria Nosratinia, *Fellow, IEEE*

***Abstract*—We investigate coded modulation for full-duplex relay channels, proposing and analyzing a multilevel coding (MLC) framework with capacity approaching performance and practical features. Sufficient conditions are derived under which multilevel coding meets the known achievable rates for decode-and-forward (DF) relaying. The effect of a bit additive superposition and the linearity of multilevel code components on the performance of the system are studied. It is shown that linearity of the relay codebook imposes no penalty on rate, however, the linearity of the source-to-relay code may impose a performance penalty especially for small modulation constellations. We show that this rate loss occurs because linearity at the source node introduces a new tension between optimality of rate allocation in multilevel coding layers and optimality of source/relay codebook correlations. Motivated by this insight, alternative modulation labelings are studied that minimize the rate loss. The results are extended to multi-antenna relays. Slow fading and fast Rayleigh fading without channel state at the transmitter are also analyzed. The error exponent of the proposed scheme is studied. Finally, the frame- and bit-error rate performance of the proposed scheme is studied via simulations using point-to-point LDPC codes, showing that the proposed MLC relaying has excellent performance.**

I. Introduction

Recent advancement in hardware design and signal processing have put full-duplex operation back on the map as a potentially viable alternative [1]–[4], and much research is on-going in the area of full-duplex link implementation [5]–[7]. The credit for this resurgence of interest goes to the new research in mitigating the so-called loop-back interference (self-interference) at the full-duplex transmitter, represented by [8]–[11] among many others.

Focusing our attention on full-duplex *relays*, we find that while early theoretical relay results were in the context of full-duplex transmission [12], subsequent coding and signal processing results have concentrated for the most part on half-duplex scenarios, in particular low-SNR (binary) signaling [13]–[15]. Exceptions do exist, e.g. lattice codes for the full-duplex relay channel [16] but a nontrivial gap to capacity remains and, in the most general setting, the problem of capacity-approaching coding and modulation for the full-duplex relay channel remains open. We address this problem via multilevel coding, providing well-defined and systematic design principles that lead to near-capacity performance.

The key advantage of multilevel coding [17], [18] is that it uses binary codes whose design is by now very well understood. Moreover, the multiple binary encoders that feed the bit-levels of the modulation can operate independently.

Further related results in the relay literature are as follows. Multilevel coding in the orthogonal relay channel was studied in [19]. Several contributions for the bandwidth limited relay channel focused on the two way relay channel. Ravindran et. al [20] studied LDPC codes with higher order modulation for the two way relay channel. Chen and Liu [21] analyzed different coded modulation transmissions for the two way relay channel. Chen et. al [22] studied multilevel coding in the two-way relay channel. Hern and Narayanan [23] studied multilevel coding in the context of compute-and-forward. However, the two-way relay channel does not consider the direct link like in the conventional relay channel, and hence, the coded modulation techniques that are considered in the literature cannot be used for the three-nodes full-duplex relay channel.

A key contribution of this paper is, first, to elucidate conditions under which multilevel coding for the relay channel achieves the constellation-constrained capacity. Second, to highlight the challenges involved in meeting this bound. Third, to propose solutions for these challenges, and demonstrate the performance of the proposed solutions. The bit-additive superposition used in this paper was introduced for the broadcast channel in [24]. A preliminary version of some of the results of this paper have appeared in a conference [25], and a related paper [26] addresses multilevel coding for the half-duplex relay channel.

We propose a simple multilevel full-duplex relay transmission. The straightforward application of multilevel coding to the relay channel would result in code specifications that require multiple inter-layer correlations between the source and relay codes. Our work produces a streamlined coding procedure where the dependencies are limited to pairwise correlation between the source/relay codes at each individual layer. Moreover, we provide a simple implementation of this idea via a binary addition between conventionally designed codes. Numerical results show that the performance of the proposed technique is almost as good as the best known decode-and-forward (DF) performance (with Gaussian codewords). We show that linearity of the source-to-relay code may impose

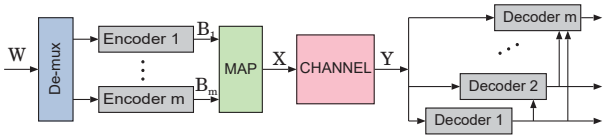

Fig. 1. MLC and MSD in point to point channel.

This work was supported in part by the grants ECCS1546969 and ECCS1711689 from the National Science Foundation.

The authors are with the Department of Electrical Engineering, the University of Texas at Dallas, Richardson, TX 75083-0688 USA, E-mail: ahmed.abotabl@utdallas.edu;aria@utdallas.edu.

a performance penalty. We propose a solution that minimizes this performance penalty using a proper labeling design. The error exponent of the proposed transmission is studied under sliding window decoding. Simulation results show that good point-to-point codes (DVB-S2 codes) produce performance that is very close to the fundamental limits when used in the proposed transmission. In addition, two methods are experimentally verified for directly approaching the performance of non-linear codes in full-duplex relays: insertion of randomly located zeros into DVB-S2 codewords (using pseudo-random generators whose seed is known at source and destination), and inserting zeros at fixed locations that are determined via a puncture optimization strategy [27], resulting in a degenerate linear code. The relative performance of the two methods is discussed.

II. Preliminaries

In the point-to-point channel, binary components multilevel coding (see Fig. 1) is implemented by splitting the data stream represented by the variable W into $m = \log_2(q)$ sub-streams for a q-ary constellation. Each sub-stream i is encoded independently with rate R_i. At each time instance, the outputs of the (binary) encoders are combined to construct the vector $[B_1, B_2, \dots B_m]$ which is then mapped to a constellation point X and transmitted over. The channel is described by the conditional distribution $P_{Y|X}(y|x)$ where Y is the output of the channel. The mutual information between the input and output is given by

$$I(X;Y) = I(B_1, B_2, \dots, B_m; Y) = \sum_{i=1}^{m} I(B_i; Y|B^{i-1}) \quad (1)$$

with the definition $B^{i-1} \triangleq [B_1, B_2, \dots, B_{i-1}]$ with B^0 representing a constant, and using the chain rule for mutual information and the one-to-one relationship between X and $[B_1, B_2, \dots, B_m]$. This equation suggests a multistage decoding where the codeword of level i is decoded using the output of the decoders of the preceding levels. A necessary and sufficient condition for multilevel coding achieving the constellation constrained capacity is that the optimal distribution $P^*_{B_1,\dots,B_m}(b_1, \dots, b_m)$ must be independent across its components [28], in other words, the optimal channel input distribution is equal to the input optimal distribution under MLC,

$$P_{B_1,\dots,B_m}(b_1, \dots, b_m) = \prod_{i=1}^{m} P_{B_i}(b_i) \quad (2)$$

Although the capacity of the full-duplex relay channel is in general unknown, we know the rates supported by several specific transmission schemes, including decode-and-forward which achieves the capacity of the degraded relay channel, partial decode-and-forward and compress-and-forward. In this paper we consider only the decode-and-forward transmission.

Due to the causality of the relay, the relay transmit a message at block t that was transmitted from the source at block $t-1$ therefore, to provide assistance to the relay, each transmission from the source depends on the message of block t as well as the message of block $t-1$ which is known as Block-Markov encoding [12]. Throughout the paper we denote the signal transmitted from the source node and the relay node in block t by $X_1^{(t)}$ and $X_2^{(t)}$. We begin by modeling the received signal at the relay, which experiences self-interference:

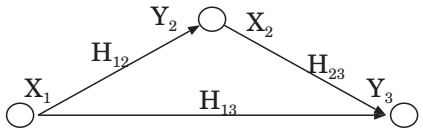

Fig. 2. Full-Duplex relay channel.

$$Y_2^{(t)} = H_{12}X_1^{(t)} + n_2 + n_s$$

where H_{12} is the channel from the source to the relay, n_2 is the additive Gaussian (thermal) noise at the receiver, and n_s is the sampled residual self-interference. The area of modeling and analyzing loop-back or self-interference has experienced rapid growth in the past few years. Several methods for mitigating self-interference are now in place, among them antenna design and placement (including passive components), as well as echo cancellation in the amplifier stage, as well as digital signal processing after down-conversion and sampling [8]. The collection of these methods have allowed the residual self-interference to be reduced significantly. The *residue* of self-interference, n_s, is the component that is seen by the relay decoder. Several works to date [8], [29], [30] have used a Gaussian model for n_s, an approximation that is confirmed by various measurements [31], [32]. Therefore, the combination $\tilde{n}_2 = n_2 + n_s$ is also Gaussian with appropriate variance.

Thus, the received signal at the relay and destination in block t are respectively given by

$$Y_2^{(t)} = H_{12}X_1^{(t)} + \tilde{n}_2 \quad (3)$$

$$Y_3^{(t)} = H_{13}X_1^{(t)} + H_{23}X_2^{(t)} + n_3 \quad (4)$$

where H_{12}, H_{13} and H_{23} are the fading channel coefficients as illustrated in Fig. 2.

The destination uses either backward decoding at which the destination waits until the reception of the last transmission block or a sliding window decoder at which the decoder uses L blocks for decoding where L is the window size [33].

III. Multilevel Decode and Forward

Subject to the channel probability distribution $P_{Y_2,Y_3|X_1,X_2}(y_2, y_3|x_1, x_2)$, the decode-and-forward achievable rate is

$$R \leq \max_{P_{X_1,X_2}(x_1,x_2)} \min\{I(X_1; Y_2|X_2), I(X_1, X_2; Y_3)\} \quad (5)$$

where the channel state information is assumed to be perfectly known in a path-loss model and slow fading model. Please note that in the ergodic channel case, the channel coefficients are implicitly included in the expression as follows:

$$I(X_1; Y_2|X_2) = \mathbb{E}_{H_{12},H_{23},H_{13}}[I(X_1; Y_2|X_2, H_{12}, H_{13}, H_{23})]$$

$$I(X_1, X_2; Y_3) = \mathbb{E}_{H_{12},H_{23},H_{13}}[I(X_1, X_2; Y_3|H_{12}, H_{13}, H_{23})]$$

The design variable of this optimization problem is the joint distribution $P_{X_1,X_2}(x_1,x_2)$. This optimization problem is hard to solve. Moreover, it leaves open the question of a *practical* encoding with codebook that meets or approximates this distribution. In this section, we address the optimization of codebook distributions in the context of multilevel coding, and also examine its consequences on the decoder side.

A. Encoding

For ease of exposition we consider the case where the source and the relay multilevel codes have the same number of levels m, a restriction that does not lead to any loss in generality as described in Remark. 3. As shown in Fig. 3, the signals X_1, X_2 at the source and the relay respectively are represented by their modulation-constrained index variables $B^m = [B_1, \ldots, B_m]$ and $C^m = [C_1, \ldots, C_m]$ respectively; The relay and the source can use different sets of encoders. The source uses block-Markov superposition, therefore C^m and B^m are dependent. This dependence can be shown in Fig. 3 through the delay operation Z^{-nR} which is a delay of one transmission block. The two inputs of each encoder at the source are the current block message and the previous block message which is assumed to be known at the relay after successful decoding in the previous block. The two messages are encoded jointly using a generic encoder defined over a finite field. A special form of this generic encoder is shown in Fig. 4. The rate in (5) is equivalent to

$$R \leq \max_{P_{B^m,C^m}(b^m,c^m)} \min\left\{I(B^m;Y_2|C^m), I(B^m,C^m;Y_3)\right\} \tag{6}$$

The design variable $P_{B^m,C^m}(b^m,c^m)$ implies that the vectors B^m and C^m can be generated with any joint distribution which implies any dependency between $[B_1,\ldots,B_m]$ and $[C_1,\ldots,C_m]$. Multilevel coding introduces an additional constraint: that the entries of the vector $[B_1,\ldots,B_m]$ should be encoded independently and $[C_1,\ldots,C_m]$ should be also encoded independently. However, the dependency between B^m and C^m is necessary for the superposition coding. This independence between the entries of B^m and C^m introduces a constraint on the optimization, resulting in the following rate:

$$R \leq \max_{\prod_{i=1}^m P_{B_i|C^m}(b_i|c^m)P_{C_i}(c_i)} \min\left\{I(B^m;Y_2|C^m) \right. \\ \left., I(B^m,C^m;Y_3)\right\} \tag{7}$$

Multilevel coding is optimal if the new constraint is not active, i.e., if the unconstrained optimization already satisfies the constraint:

$$P^*_{B^m,C^m}(b^m,c^m) = \prod_{i=1}^m P^*_{B_i|C^m}(b_i|c^m)P^*_{C_i}(c_i) \tag{8}$$

where $P^*()$ is the optimal distribution.

So far we borrowed ideas from the point-to-point channel [34], but this is not enough to produce a multilevel scheme in the usual sense for the relay channel, because the cross-dependence of the source and relay transmissions still binds the source streams together. In other words, the source streams up to this point are only *conditionally* independent. We now proceed to address this issue via a framework allowing each level of the source signal to depend on the relay signal *only at the same level*, i.e., allowing each B_i to depend only on C_i. Then the achievable rate is

$$R \leq \max_{\prod_{i=1}^m P_{B_i|C_i}(b_i|c_i)P_{C_i}(c_i)} \min\left\{I(B^m;Y_2|C^m), \right. \\ \left. I(B^m,C^m;Y_3)\right\} \tag{9}$$

A sufficient condition for this to be capacity optimal is:

$$P^*_{B_i|C^m}(b_i|c^m) = P^*_{B_i|C_i}(b_i|c_i) \qquad \forall i \tag{10}$$

It remains an open question exactly which channels and which modulations satisfy this sufficient condition. However, in this work we show via numerical results that this approach produces rates that are close to the constellation constrained capacity.

Remark 1: For generality, the mutual information expressions in this section do not show explicit dependence on channel statistics. For additive Gaussian channels, Y_2 and Y_3 depend on the input variables via AWGN. In a pure line-of-sight model, the dependence is via a path loss exponent and AWGN. We consider first a path loss model with AWGN to explain the main ideas of the proposed work while a generalization of our work to the slow fading and fast fading cases are studied in the sequel.

Remark 2: Coded modulation for the relay is attempting to implement a Gaussian codebook, which for the decode-and-forward consists of a superposition whose cloud centers are the relay codebook, and the satellites are the source codebook. The cloud centers are transmitted cooperatively to the destination. The satellite codewords (conditioned on the cloud center) send the relay the new information for the next transmission block. To implement this cooperative transmission, the source and the relay may use either the same modulation or two modulations from the same family (for example 16QAM and 64QAM).

Remark 3: The expressions above were developed for identical modulation constellation at the source and the relay. These expressions can be modified without difficulty to apply to two different modulations of the same modulation family by forcing certain B_i or C_i to be trivial random variables (constant).

B. Multistage decoding

Multistage decoding is simpler than joint decoding and is optimal in the point-to-point channel [34]. To investigate this issue in the relay channel, we focus on the decoding requirement at both the relay and the destination. For relay decoding, we must have at each level i:

$$R_i \leq I(B_i;Y_2|B^{i-1},C^m) \tag{11}$$

So the relay is able to do multistage decoding in a straightforward matter. At the destination, the multistage decoding depends on the two possible relaying strategies [12]: in the first strategy, the relay transmits a hash at a rate supported by the relay-destination link (with partial interference from source considered as noise). The destination first decodes the hash and

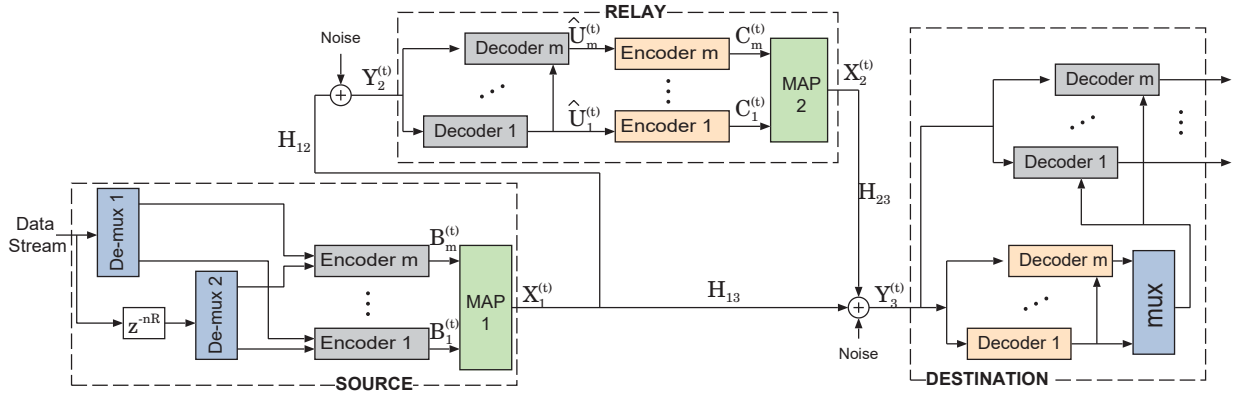

Fig. 3. MLC and MSD in the Relay channel with regular successive decoding

then the overall received signal is decoded with the help of the hash. In this case, the destination successively decodes the relay signal and then the source signal (Fig. 3) which requires the rates to satisfy:

$$R_i \le I(B_i; Y_3|B^{i-1}, C^m) \tag{12}$$

$$R_{ri} \le I(C_i; Y_3|C^{i-1}) \tag{13}$$

where R_{ri} is the rate of level i at the relay. Combining the rate constraints we obtain

$$R \le \max_{\prod_{i=1}^m P_{B_i|C_i}(b_i|c_i)P_{C_i}(c_i)} \min\left\{ \sum_{i=1}^m I(B_i; Y_2|C^m, B^{i-1}), \sum_{i=1}^m I(C_i; Y_3|C^{i-1}) + I(B_i; Y_3|B^{i-1}, C^m) \right\} \tag{14}$$

In the second strategy, the relay codebook has rate that may be above the capacity of the relay-destination link, but is still decodable at the destination when joined with the source signal. The multistage version of this joint decoding is shown in Fig. 4 and requires the individual levels to obey the following rate constraints:

$$R \le \max_{\prod_{i=1}^m P_{B_i|C_i}(b_i|c_i)P_{C_i}(c_i)} \min\left\{ \sum_{i=1}^m I(B_i; Y_2|C^m, B^{i-1}), \sum_{i=1}^m I(B_i, C_i; Y_3|B^{i-1}, C^{i-1}) \right\} \tag{15}$$

Both (14) and (15) result in the same overall rate. However, level-wise rate allocations will be different according to the different strategies.

IV. Code Design

Fig. 4 shows a block diagram of multilevel encoders and multistage decoders according to the principles outlined in the previous sections. The data is fed into the encoder in blocks of size k. Each block-Markov transmission is dependent on two successive data blocks. These two data blocks (the present and the past) are demultiplexed into levels V_i and U_i, respectively. At each level i, the two data components are encoded via superposition coding (not necessarily with XOR operation as shown in Fig. 4) to produce the mapping indices B_i. $\hat{V}_i$ represents the relay's estimate of V_i which is correct under decode-and-forward. C_i is the level-i relay codeword, whose data word U_i is known via relay reception at time $t-1$, i.e., $V_i^{(t)} = U_i^{(t-1)}$.

A. Bit additive superposition

For superposition we propose to use a modulo-2 addition of constituent binary codes for each level (Bit additive), see [33, Chapter 5] and [35]. The result is shown in Fig. 4, where for each level i the demultiplexed data streams U_i and V_i are separately encoded into C_i and F_i, respectively, and then the input to the modulation mapper is obtained by $B_i = C_i \oplus F_i$. The achievable rates under this condition can be characterized by:

$$R \le \max_{\prod_{i=1}^m P_{B_i|C_i}(b_i|c_i)P_{C_i}(c_i)} \min\left\{ \sum_{i=1}^m I(B_i; Y_2|C^m, B^{i-1}), \sum_{i=1}^m I(B_i, C_i; Y_3|B^{i-1}, C^{i-1}) \right\}$$
$$\text{subject to } P_{B_i|C_i}(b_i|c_i) = P_{B_i|C_i}(\bar{b}_i|\bar{c}_i) \tag{16}$$

The constraint $B_i = C_i \oplus F_i$ for some Bernoulli random variable F_i is equivalent to the constraint $P_{B_i|C_i}(b_i|c_i) = P_{B_i|C_i}(\bar{b}_i|\bar{c}_i)$ on the distribution of B_i, C_i, where $\bar{b}_i$ denotes the logical complement of b_i. Clearly this is a restrictive constraint as it reduces the degrees of freedom in the joint distribution of B_i, C_i. However, as will be shown in the sequel, this superposition structure does not induce a rate penalty.

Subsequently, we introduce a linearity constraint on the code with code bits C_i [1]. Subject to this new constraint, the achievable rate will be:

$$R \le \max_{\prod_{i=1}^m P_{B_i|C_i}(b_i|c_i)P_{C_i}(c_i)} \min\left\{ \sum_{i=1}^m I(B_i; Y_2|C^m, B^{i-1}), \sum_{i=1}^m I(B_i, C_i; Y_3|B^{i-1}, C^{i-1}) \right\}$$
$$\text{subject to } P_{B_i|C_i}(b_i|c_i) = P_{B_i|C_i}(\bar{b}_i|\bar{c}_i)$$

[1] A code is linear when the codewords constitute a vector space.

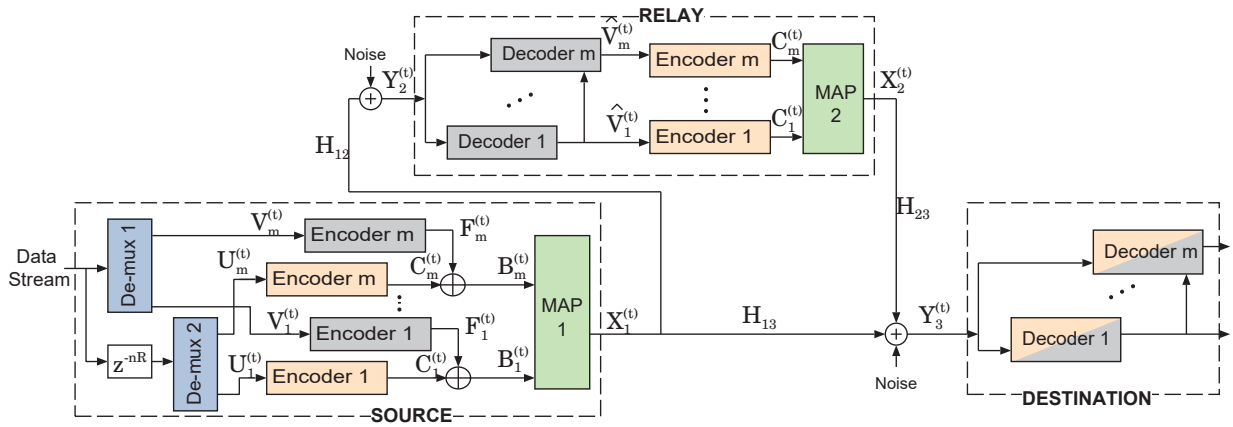

Fig. 4. MLC and MSD in the Relay channel with level by level decoding

$$P_{C_i}(1) = \frac{1}{2} \tag{17}$$

The constraint $P_{C_i}(1) = \frac{1}{2}$ restrict all the possible distributions of C_i to those only that will result in a linear code. Once again, numerical results show that this new constraint introduces no rate penalty. Finally, we consider the case where all codes are linear and full-rank (The generator matrix of the code is full-rank). Then the achievable rates are obtained via:

$$\begin{aligned} R \leq \max_{\prod_{i=1}^{m} P_{B_i|C_i}(b_i|c_i)P_{C_i}(c_i)} & \min\left\{ \sum_{i=1}^{m} I(B_i; Y_2|C^m, B^{i-1}), \right. \\ & \left. \sum_{i=1}^{m} I(B_i, C_i; Y_3|B^{i-1}, C^{i-1}) \right\} \\ \text{subject to } & P_{B_i|C_i}(b_i|c_i) = P_{B_i|C_i}(\bar{b}_i|\bar{c}_i) \\ & P_{C_i}(1) = \frac{1}{2} \\ & P(B_i = C_i) \in \{\frac{1}{2}, 1\} \end{aligned} \tag{18}$$

The last constraint enforces that B_i, C_i must be either independent or equal. The last two constraints in (18) restrict all the possible distributions of C_i and F_i to those that are compatible with linear codes. If the optimization results in a level i having $b_i = c_i$, it means that level i is only used to help the relay-destination transmission through increasing the correlation between X_1 and X_2, and carries no new information for the relay. Case studies show that Eq. (18) may introduce a nontrivial rate penalty compared with (17), especially in lower-order modulations (Fig. 5).

Remark 4: We introduced constraints one-by-one to shed light on exactly which one of the practical constraints introduces rate loss. It so happens that both the XOR superposition as well as linearity of the relay code are harmless, but introducing linearity in both codes in certain cases has a cost.

The behavior of linear codes and XOR superposition structure can be explained as follows: To begin with, assume that the source, relay and destination are all on one line where the distance between the source and the destination is 4 and that the distance between the source and the relay is d. When d is negative this means that the source node is between the relay and the destination and when d is positive this means that the relay is between the source and destination. In order to simply show the effect of XOR superposition and linearity, assume only a path-loss channel model with path-loss exponent $\alpha = 2$. Fig. 5 shows that linearity of the codes induces no rate loss when the relay is close to the destination. These are locations where source-relay link is the bottleneck and therefore the correlation between the source signal and the relay signal is not highly important. Conversely, when the relay is far from the destination and close to the source, the source should help the relay transmission to the destination, and hence, high correlation is required, and in that regime Fig. 5 shows linear codes can induce a rate loss, which we explain and analyze below.

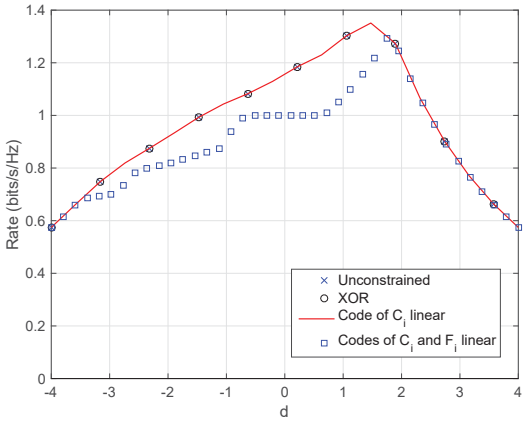

Fig. 5. Rate penalty due to linearity of F_i vs. relay location d. XOR superposition and linearity of C_i induce no rate penalty.

The linearity of the binary code implies that the symbols are zero and one with equal probability, except for the trivial all-zero code. When F_i is always equal to zero, level i does not transmit any information to the relay. When F_i is either one or zero with a uniform distribution, B_i is independent of C_i. Therefore, under linear codes each level i can be used for only one of two purposes: either it transmits data to the relay, or it is used to help the relay transmission toward the destination via correlation , but not both. So at each level, we must either

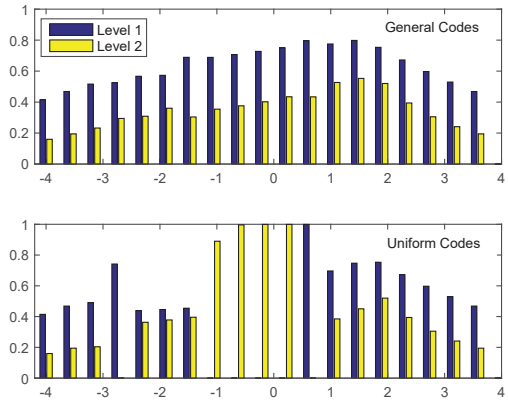

Fig. 6. 4-PAM relay level-wise rate allocation for unconstrained (top) and linear codes (bottom) as a function of relay location d under natural labeling. Source-destination distance is 4, transmit powers are 10dB.

give up the perfect allocation of rate to the relay, or give up correlation. This tension, which does not exist with nonlinear codes, gives rise to the rate loss in linear codes especially at low-order modulations. Fig. 6 shows this phenomenon in 4-PAM constellation under the same model considered earlier as explained as follows:

The figure displays the source-relay rate from each individual level of the 4-PAM constellation under the two cases of general codes and uniform codes. It is observed that under general codes, each level transmits some information to the relay. However, under linear codes, and specially when the relay is close to the source (correlation is needed), one level does not provide any source-relay rate. This is because these levels are dedicated for correlation. The zero-rate assignment to some levels in this figure are due to the uniform distribution constraint that forces each level to either send new information to the relay or assist the relay-destination transmission. Because of interference between the levels, the optimal strategy might abruptly change with small changes in the channel gains.

Remark 5: When the modulation order is large compared with the capacity of the channel, this effect is much reduced. The reason is that the rate allocated to some layers will be small, therefore it is possible to use those layers purely for correlation without a loss of efficiency for transmission to the relay. This insight will be used subsequently to design labelings that reduce the rate loss.

B. Labeling Design For Linear Coding

Linear codes constrain the marginal distributions that can be supported, which may not include (or be close to) the optimum.The idea of this section is to select a modulation labeling whose corresponding (optimal) input distributions is as close to uniform as possible, and therefore are suitable for use with linear codes.[2]

[2]The design of labeling can also be achieved via a set-partitioning methodology. More specifically, the labeling design in this section can be expressed in terms of equivalent set partitions, but is omitted in the interest of brevity and compatibility with the analytical methods of this paper.

$[\rho_1, \rho_2]$	[0,0]	[0,1]	[1,0]	[1,1]
Natural {00,01,10,11}	0	0.2	0.8	1
Gray {00,01,11,10}	0	0.19	0.79	1
Custom {00,11,10,01}	0	0.41	0.51	1

TABLE I
CORRELATION VIA LINEAR CODES. THE LABELS CORRESPOND TO SUCCESSIVE 4-PAM CONSTELLATION POINTS.

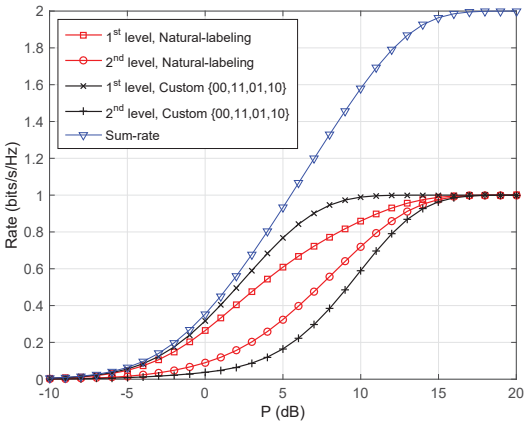

Fig. 7. The point-to-point achievable rate for 4-PAM under different labelings

The bit-additive structure under linear coding admits 2^m different correlations;[3] examples for 4-PAM are shown in Table I where ρ_i is the correlation between level i at the source and level i at the relay. This table shows the correlation of 4-PAM source/relay codewords when each of the two levels of 4-PAM are either fully correlated or uncorrelated, as required by linear codes. The label sets are assigned sequentially to 4-PAM constellation symbols. The corresponding source-relay rates are shown in Fig. 7.

The two parameters in the labeling that determine the total transmission rate are the correlation achieved by each level (if the level is used for correlation) and the source-relay rate through each level (if the level is used for sending new information to the relay). For ease of exposition we consider a source-relay code implemented using a 4-PAM modulation. The two parameters discussed earlier are the available point-to-point (source-relay) rate shown in Fig. 7 for different labelings and the available values of the correlation given in Table. I.

Therefore, if the position of the relay requires a modest amount of assistance, there are two cases. Firstly, if the source-relay SNR is very high, the achievable rates of both levels for the two different labelings is almost the same. From Table. I, it is shown that the maximum correlation other than one[4] can be obtained by using natural labeling and assigning the most significant bit for full correlation. Secondly, as the relay moves far from the source, the SNR value at the relay goes down (which leads to difference in the levels between the

[3]Because at each level, the bit-additive linear codes can produce correlation zero or one.

[4]Maximum correlation between the source and the relay cannot be one because this means that zero rate will be transmitted to the relay node, leading to zero total transmission rate.

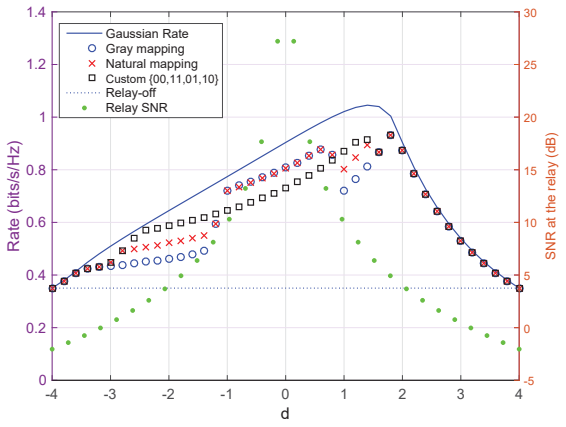

Fig. 8. Multilevel coding transmission rate for different labelings, $P_1 = P_2 = 10$dB

natural labeling and the custom labeling) and the required value of the correlation between the source and the relay also goes down. To accommodate source-relay rate, it is better to use the custom labeling and assign the least significant bit for correlation because it already has a small rate penalty compared to natural labeling. Table. I shows that assigning the least significant bit of the custom labeling for correlation will provide higher correlation than that of the natural labeling.

As explained earlier, there are also cases where the correlation is unimportant (e.g. relay very close to destination) in which case either of the labelings will perform the same.

To illustrate the effect of the choice of labeling on the performance of linear codes, we use again the 4-PAM modulation with the three labelings shown in Table I. The throughput of a decode-and-forward relay is optimized subject to these labelings and under a linear coding constraint, with the results shown in Fig. 8, assuming the same system model with d_{13}=4.

Several different regions of operation clearly stand out. First, when relay is close to the destination, correlation between the source and relay is not required and in fact linear coding does not incur a rate penalty. For other source-relay-destination configurations, either a natural labeling or the custom labeling performs best.

Remark 6: We observe that the Gray labeling is never the best labeling in 4-PAM MLC in the relay channel. This is because the mutual information curves for Gray labeling are exactly the same as natural labeling, however, Gray labeling produces smaller correlation than natural labeling. We also observe that natural and Gray labeling perform very well for $-1 < d < 1$. This is because in this setting, the relay is so close to the source which makes the multiple-access phase to be the bottleneck of the transmission. Therefore, high correlation between the source and the relay is required. Table I shows that natural and Gray labeling can provide higher source-relay correlation.

Remark 7: In this Section, it was assumed that the same modulation constellation is used at the source and the relay, including the labeling. A non-identical labeling will interfere with the level-wise correlation and does not confer any obvious advantages.

Remark 8: Optimization of labeling can be performed via exhaustive search for small constellations. For large constellations, as mentioned earlier, the performance penalty of linear codes is vanishingly small (due to availability of a large set of feasible correlation values), therefore any labeling (e.g. natural labeling) works well and there is no need for optimizing the labeling.

C. Slow Fading Relay Channel

In this section, we consider that the channel coefficients are fixed over each transmission block and the channel state information is known at the receiver (CSIR). In this case, the information that can be transferred form the source node to the destination node is

$$I = \min\{I(X_1; Y_2|X_2, H_{12}), I(X_1, X_2; Y_3|H_{23}, H_{13})\} \tag{19}$$

and the mutual information between level i at the source and level i at the destination is

$$\begin{aligned} I_i = \min\{&I(B_i; Y_2|B^{i-1}, X_2, H_{12}), \\ &I(B_i, C_i; Y_3|B^{i-1}, C^{i-1}, H_{23}, H_{13})\} \end{aligned} \tag{20}$$

Assuming that the transmission rate of level i is R_i, the outage event of level i is $I_i < R_i$. The outage probability is then given by

$$P_{outage} = \bigcup_i Pr(I_i < R_i) \leq \sum_i Pr(I_i < R_i) \tag{21}$$

where the last inequality is from the union bound. Each of the mutual information I_i can be calculated numerically in a similar manner to the curves in Fig. 7.

D. Fast Fading Relay Channel

In this section, we show the applicability of our analysis and design to the Rayleigh fading channel with channel state at the receivers. Assume that the fading coefficient between node i and node j is H_{ij}. The three channel gains are all independent and identically distributed with a normal distribution $\mathcal{N}(0, 1)$. In this case, the decode-and-forward transmission rate is

$$\begin{aligned} R \leq \max_{P_{X_1,X_2}(x_1,x_2)} \min\big\{&\mathbb{E}_{H_{12}}\big[I(X_1; Y_2|X_2, H_{12})\big], \\ &\mathbb{E}_{H_{13},H_{23}}\big[I(X_1, X_2; Y_3|H_{13}, H_{23})\big]\big\} \end{aligned} \tag{22}$$

where $\mathbb{E}$ is the expectation operator. Therefore, the multilevel decomposition in (16) is still valid, given the following averaging over the channel coefficients:

$$I(B_i; Y_2|C^m, B^{i-1}) = \mathbb{E}_{H_{12}}\big[I(B_i; Y_2|C^m, B^{i-1}, H_{12})\big] \tag{23}$$

$$\begin{aligned} &I(B_i, C_i; Y_3|B^{i-1}, C^{i-1}) \\ &\quad = \mathbb{E}_{H_{13},H_{23}}\big[I(B_i; Y_2|C^m, B^{i-1}, H_{13}, H_{23})\big] \end{aligned} \tag{24}$$

The code design criteria described earlier depends on prior knowledge of the point-to-point mutual information curves

in Fig. 7 and the correlation supported by each level in Table I. These metrics will change in a fading environment however, it can be easily obtained by averaging over the normally distributed fading coefficient. Having reached to these quantities, the design will follow directly the same steps described earlier.

E. Multi-antenna Relay

Assume that the relay node has N receive antennas and M transmit antennas. Also, assume that the channel state is known at all nodes. The bold letters in this subsection represent the vector version of the variable. In this subsection, we show that the proposed multilevel transmission and code design follows directly in this case. We start with the source relay transmission. The only difference in this case is that the relay receives multiple versions of the transmitted symbol and can combine them with any of the existing techniques such as maximum ratio combining. The transmission rate from the source to the relay in this case becomes

$$R_{SR} \leq I(X_1; \boldsymbol{Y}_2 | \boldsymbol{X}_2, H_{12}^{(1)}, \ldots, H_{12}^{(N)}) \quad (25)$$

$$= I(B^m; \boldsymbol{Y}_2 | \boldsymbol{X}_2, H_{12}^{(1)}, \ldots, H_{12}^{(N)}) \quad (26)$$

$$= \sum_{i=1}^{m} I(B_i; \boldsymbol{Y}_2 | \boldsymbol{X}_2, B^{i-1}, H_{12}^{(1)}, \ldots, H_{12}^{(N)}) \quad (27)$$

which implies that the transmission rate of level i at the source is upper bounded by

$$R_i \leq \sum_{i=1}^{m} I(B_i; \boldsymbol{Y}_2 | \boldsymbol{X}_2, B^{i-1}, H_{12}^{(1)}, \ldots, H_{12}^{(N)}) \quad (28)$$

Now, we show that the relay-destination transmission can be modeled as a single antenna transmission. Assume that the channel from the ith antenna at the relay node to the destination node is $H_{23}^{(i)}$. To show that the system can be modeled as a single antenna relay, we assume a Gaussian input relay channel. The relay can use the M transmit antennas to provide power gain by sending the same signal X_2 from all the antennas. Assuming that the transmit power of each antenna is $P_2^{(i)}$, we have the following constraint

$$\sum_{i=1}^{M} P_2^{(i)} \leq P_2. \quad (29)$$

The received signal at the destination is

$$Y_3 = \sum_{i=1}^{m} H_{23}^{(i)} \sqrt{P_2^{(i)}} X_2 + H_{13} \sqrt{P_1} (X_1 + X_2) + n_3 \quad (30)$$

$$= (\sum_{i=1}^{m} H_{23}^{(i)} \sqrt{P_2^{(i)}} + H_{13} \sqrt{P_1}) X_2 + H_{13} \sqrt{P_1} X_1 + n_3 \quad (31)$$

which is equivalent to single antenna relay channel where the channel gain from the relay to the destination is

$$\sum_{i=1}^{m} H_{23}^{(i)} \sqrt{P_2^{(i)}} + H_{13} \sqrt{P_1}. \quad (32)$$

This requires an optimization over the powers of the transmit antenna at the relay however, once the power allocation is optimized, the problem becomes similar to the single relay antenna transmission.

V. Error Exponent Analysis

In a point-to-point channel, the error exponent upper bound takes the form

$$P_e \leq e^{-nE(R)} \quad (33)$$

where n is the blocklength and $E(R)$ is the error exponent as a function of the transmission rate. In this section we derive an upper bound error exponent for the proposed transmission and compare it with the error exponent of the channel with no restrictions on the input. The error exponent of the full-duplex decode and forward relay channel was studied by Li and Georghiades [36] under backward decoding. Bradford and Laneman studied the error exponent of the full-duplex relay channel under sliding window decoding [37]. Tan [38] produced the full-duplex relay error exponent for partial decode and forward and compress and forward under backward decoding. We study the error exponent of multilevel coding in full-duplex relay under sliding window decoding; the backward decoding analysis is similar and is omitted for brevity.

The error event in the relay channel has two components, the decoding error at the relay and the decoding error at the destination node. An error at the relay node will lead to an error at the destination with very high probability. For the sake of clarity, we need to define two error probabilities at each node, ϵ_R is the probability of error at the relay given that the previous block was decoded successfully and ϵ_D is the probability of error at the destination given that the current block is decoded successfully at the relay and the previous block is decoded successfully at the destination. These error probabilities are defined conditioned on a previously successful decoding to simplify the analysis. It was shown by Bradford and Laneman [37] that the probability of error in the full-duplex relay communications can be upper bounded by

$$P_e \leq (B-1)(\epsilon_R + \epsilon_D) \quad (34)$$

where B is the number of blocks.

Since each probability of error at each node has an associated error exponent that determines an upper bound on the probability of error, each error probability can be upper bounded by it's error exponent. This leads to the random coding error exponent of the entire transmission,

$$E(R) \geq \frac{1}{B} \min\{E_R(R), E_D(R)\} - \frac{\log 2(B-1)}{D} \quad (35)$$

where $E_R(R)$ and $E_D(R)$ are the random coding error exponents corresponding to ϵ_R and ϵ_D respectively and D is the total number of transmission symbols in the B blocks ($D = nR$) where n is the blocklength.

In the rest of this section, for the sake of completeness we state the error exponents in (35) for the probability of error at each node under no encoding restriction. Consequently,

we present the same error exponents under multilevel coding and finally for the multilevel coding with multistage decoding. In the following, for brevity and clarity of exposition, probability distributions are distinguished by their respective arguments. Recall that superscripted variables are vectors (e.g. $B^m = [B_1, \ldots, B_m]$ and $b^{i-1} = [b_1, \ldots, b_{i-1}]$). Summations are over the entire defined range of their subscript variable (or vector).

The error exponent for the probability of error at the relay, $E_R(R)$, is given by

$$E_R(R) = \max_{P(x),\rho_e} [E_{01}(\rho_e, P(x)) - \rho_e R] \tag{36}$$

where ρ_e is the random coding error exponent tilting parameter and

$$E_{01} = - \log \sum_{x_2} \int P(x_2) \Big[\sum_{x_1} P(x_1|x_2) P(y_2|x_1, x_2)^{\frac{1}{1+\rho_e}} \Big]^{1+\rho_e} dy_2 \tag{37}$$

In order to obtain the error exponent of the proposed multilevel encoding, we replace X_1 and X_2 by B^m and C^m and using the independence between the components of B^m and C^m, we find

$$E_{01} = - \log \sum_{c^m} \int \prod_i P(c_i) \times \Big[\sum_{b^m} \prod_j P(b_j|c_j) P(y_2|b^m, c^m)^{\frac{1}{1+\rho_e}} \Big]^{1+\rho_e} dy_2 \tag{38}$$

For error exponent under multistage decoding, we consider the decoding of each B_i at the receiver subject to successful decoding of the previous stages. Thus, each decoder can be thought of as operating on a channel with input B_i, output Y_2, and state B^{i-1}. Ingber and Feder [39] derived a random coding error exponent for channels with side information at the receiver

$$E(\rho_e) = - \log \mathbb{E}[2^{-E^s(\rho_e)}], \tag{39}$$

where s is the state of the channel. Similarly, Calculating the error exponent under multistage decoding at level i requires averaging over B^{i-1} since at level i, the decoder knows the outputs B^{i-1} of the preceding decoders. Therefore, E_{01} of level i is given by

$$E^i_{01} = - \log \sum_{c^m, b^{i-1}} \int P(c^m, b^{i-1}) \Big[\sum_{b_i} P(b_i|c^m, b^{i-1}) P(y_2|b^m, c^m)^{\frac{1}{1+\rho_e}} \Big]^{1+\rho_e} dy_2 \tag{40}$$

Now, we are left with combining the error exponents in all the levels to obtain E_{01} under multistage decoding. In a point-to-point channel, Ingber and Feder derived a random coding error exponent of multilevel coding and multistage decoding as a function of the error exponent of the individual sub-channels *with state known at the receiver* as mentioned earlier [34, Theorem 3]. The main idea is that the total error exponent is dominated by the minimum error exponent of all the levels. Inspired by their bound, the error exponent of the decoder at the relay $E_R(R)$ under multistage decoding is

$$E_R^{MSD}(R) = \max_{R_i, P(b_i,c_i) \forall i} \min_l \max_\rho [E^l_{01} - \rho_e R_l] \tag{41}$$

The error exponent at the destination, $E_D(R)$, is more complicated as it involves sliding window decoding. Bradford and Laneman [37] decomposed this error exponent to rely on the window size L and two other metrics, namely

$$E_0(\rho_e, P(x_1, x_2)) = - \log \int \Big[\sum_{x_1, x_2} P(x_1, x_2) P(y_3|x_1, x_2)^{\frac{1}{1+\rho_e}} \Big]^{1+\rho_e} dy_3 \tag{42}$$

$$E_{02}(\rho_e, P(x_1, x_2)) = - \log \sum_{x_2} \int P(x_2) \Big[\sum_{x_1} P(x_1|x_2) P(y_3|x_1, x_2)^{\frac{1}{1+\rho_e}} \Big]^{1+\rho_e} dy_3 \tag{43}$$

Obtaining these two parameters for the proposed multilevel transmission will require replacing X_1 and X_2 with B^m and C^m respectively to give

$$E_0(\rho_e, P(b^m, c^m)) = - \log \Bigg[\int \Big[\sum_{b^m, c^m} P(b^m, c^m) P(y_3|b^m, c^m)^{\frac{1}{1+\rho_e}} \Big]^{1+\rho_e} dy_3 \Bigg] \tag{44}$$

$$E_{02}(\rho_e, P(b^m, c^m)) = - \log \Bigg[\sum_{c^m} \int \prod_i P(c_i) \Big[\sum_{b^m} \prod_j P(b_j|c_j) P(y_3|b^m, c^m)^{\frac{1}{1+\rho_e}} \Big]^{1+\rho_e} dy_3 \Bigg] \tag{45}$$

Under multistage decoding, B^{i-1} will be decoded and passed to decoder i before it starts decoding B_i. Therefore, the error exponent should be averaged over B^{i-1} in (44) and (45) to evaluate the error exponent while decoding level i. This gives

$$E^i_0(\rho_e, P(b^m, c^m)) = - \log \sum_{b^{i-1}} \int \Big[\sum_{b_i, c^m} P(b^i, c^m|b^{i-1}) P(y_3|b^i, c^m)^{\frac{1}{1+\rho_e}} \Big]^{1+\rho_e} dy_3$$

$$E^i_{02}(\rho_e, P(b^m, c^m)) = - \log \sum_{c^m, b^{i-1}} \int P(c^m, b^{i-1}) \Big[\sum_{b_i} P(b_i|c^m, b^{i-1}) P(y_3|b^i, c^m)^{\frac{1}{1+\rho_e}} \Big]^{1+\rho_e} dy_3$$

We now numerically compare the error exponent of the proposed transmission under multistage decoding with the general error exponent of the channel with no restrictions on the encoding or decoding. These results were obtained by exhaustive search over the input distributions $P_{B_i|C_i}(b_i|c_i)$ and $P_{C_i}(c_i)$ and the tilting parameter ρ_e to find the maximum error exponent. Please note that the random variables B_i and

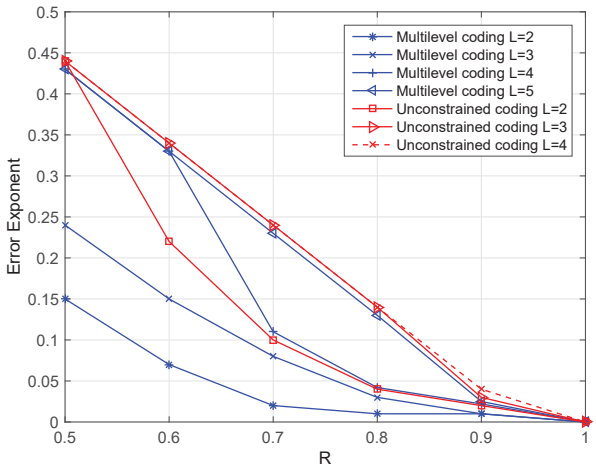

Fig. 9. Error exponent for bit-additive MLC versus unconstrained coding for 4-PAM. $P = 10$dB, $d = 1$

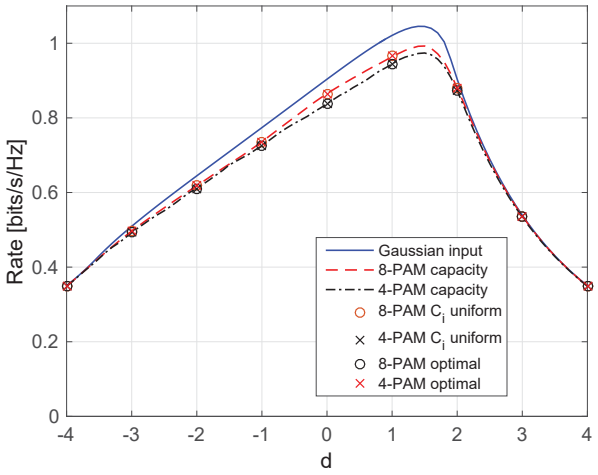

Fig. 10. Natural labeling, PAM, $P_1 = P_2 = 10$dB

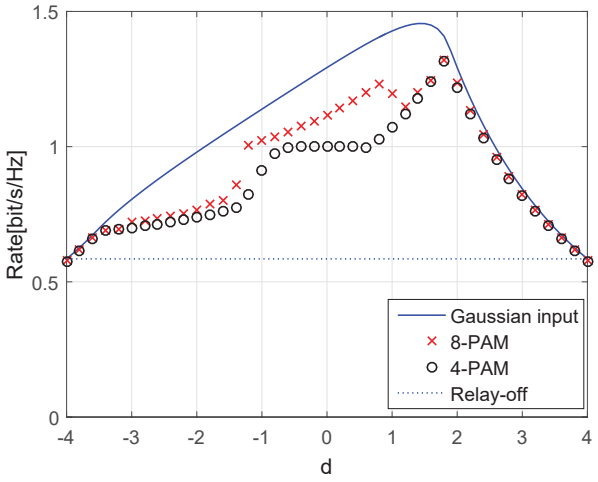

Fig. 11. Rate of multilevel transmission when using linear codes for 4-PAM and 8-PAM constellations, $P_1 = P_2 = 13$dB

C_i are binary random variables, so the optimization of each distribution is just over one parameter taking values in $[0, 1]$. For the case with no restriction on the encoding or decoding, the error exponent was found by exhaustive search over the input constellation distribution which requires significantly more computation. Fig. 9 shows the error exponent of the proposed multilevel transmission under multistage decoding at the relay and destination under 4-PAM constellation. The figure shows that when the window size increases, the error exponent of the proposed transmission gets closer to that of the general encoding at the source and relay nodes.

VI. Simulations

A. Modulation Constellations & Achievable Rates

We assume equal transmit power and the source and the relay nodes, $P_1 = P_2 = P$, and unit variance noise at the relay and destination. The noise power at the relay node includes the thermal noise and the residual self-interference. To demonstrate the performance of the relay channel in a variety of link SNRs, we assume a path loss model following the setting of the well-known work of Kramer et al [40], with a path loss exponent $\alpha = 4$. The source, relay and destination are aligned on a line, with source-destination distance d_{13}, source-relay distance d, and relay-destination distance $d_{23} = d_{13} - d$. In our simulations we take $d_{13} = 4$. The link gains are therefore $h_{ij} = (\frac{1}{d_{ij}})^{\alpha/2}$.

The figures also include, for comparison purposes, the achievable rates for the unconstrained Gaussian relay channel:

$$R_{DF} = \max_{0\le\rho\le 1} \min\left\{\frac{1}{2}\log\left(1+|H_{12}|^2P_1(1-|\rho|^2)\right),\right.$$
$$\left.\frac{1}{2}\log\left(1+|H_{13}|^2P_1+|H_{23}|^2P_2+2\rho\sqrt{|H_{13}|^2P_1|H_{23}|^2P_2}\right)\right\}$$

The transmission rates of the proposed multilevel coding are shown in Fig. 10. The transmission rates were obtain by exhaustive search over the input distribution to obtain the maximum achievable rate. The results show that the gap between the transmission rate of the proposed transmission and the Gaussian input transmission rate is very small and gets smaller with larger constellation size. The gap is smaller when the relay is far from the source and the source-relay link has smaller SNR.

Fig. 11 shows the degradation in the achievable rates when the source is enforced to use linear component codes. This implies that in the full-duplex relay, the achievable rates are sensitive to the correlation, which is unlike the half-duplex relay case reported in [41]. The 8-PAM constellation achieves significantly higher rates when the relay is close to the source, where the signaling calls for strong correlation, because the 8-PAM has a bigger set of feasible correlations under the linear coding constraint.

B. Error Rate Simulations

The DVB-S2 LDPC codes are used as component codes for each of the levels at the source node and the relay node to examine the performance of the proposed multilevel transmission. The rates of the LDPC codes are chosen according

to the design criteria in Section IV. The blocklength of the component codes is $n = 64$k. Both the relay and destination nodes used belief propagation decoding at each level where the maximum number of iterations is set to 50.

The decoding at the relay node is performed as follows: While decoding level i of the signal X_1 at the relay, the relay knows two parts of X_1 already. The first is the vector U^m which is the cloud center of X_1 and the second is the vector V^{i-1} which is the output of the preceding decoders, assuming correct decoding. Therefore, the LLR of level i at the relay is

$$LLR_r = \log \frac{P(y_2|u^m, v^{i-1}, 0)}{P(y_2|u^m, v^{i-1}, 1)} \tag{46}$$

where

$$P(y_2|u^m, v^{i-1}, v_i) = \frac{1}{P(u^m, v^{i-1}, v_i)} \sum_{v_{i+1}^m} P(y_2|u^m, v^m)$$

The decoding at the destination node is performed as follows: Assuming that the destination node will decode the signal from the relay node and then decode the signal from the source node, the LLR of level i of the relay at the destination node is

$$LLR_{RD} = \log \frac{P(y_3|c^{i-1}, 0)}{P(y_3|c^{i-1}, 1)} \tag{47}$$

where

$$P(y_3|c^{i-1}, c_i) = \frac{1}{P(c^{i-1}, c_i)} \sum_{b^m, c_{i+1}^m} P(y_3|b^m, c^m)$$

The next step is to decode the signal from the source given the transmitted signal from the relay with

$$LLR_{SD} = \log \frac{P(y_3|c^m, b^{i-1}, 0)}{P(y_3|c^m, b^{i-1}, 1)} \tag{48}$$

where

$$P(y_3|c^m, b^{i-1}, b_i) = \frac{1}{P(c^m, b^{i-1}, b_i)} \sum_{b_{i+1}^m} P(y_3|b^m, c^m)$$

and C^m carries all the information about the cloud center of the source signal.

In each of the error plots, a capacity threshold is marked that corresponds to the relay constellation constrained capacity in each case. The source and relay powers are identical throughout all simulations, enabling the use of a single scale for power (dB) in the error curves. In each of the simulations, the rates at each level are found by exhaustive search so that the sum-rate is maximized.

Fig. 12 shows the bit error probability and frame error probability for 4-PAM multilevel transmission at $d_{12} = 1$ and $\alpha = 2$. The figure shows the performance of the three labelings shown in Table I. The total transmission rate is $R = 0.8$. In general, for each labeling, the bit-wise correlation is not the same. However, for the current channel parameters, the bit wise correlations used in these simulations were $\rho_1 = 0$ and $\rho_2 = 1$ which means that the least significant bit provides assistance to the relay transmission via correlation and the most significant bit sends new information to the relay.

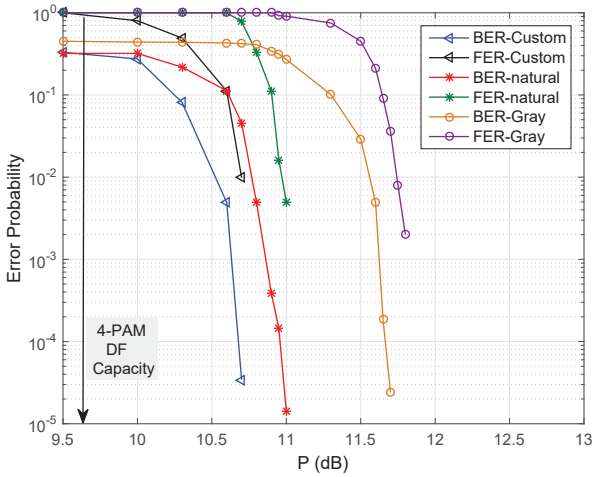

Fig. 12. Performance of Multilevel superposition for 4-PAM constellation with source-relay distance = 1

Fig. 13 shows the bit error probability and frame error probability of 8-PAM multilevel transmission at $d_{12} = 2.5$ with $\alpha = 4$. The total rate transmitted from the source node to the destination node is $R = 2.28$. The optimal value of the bit-wise correlations using linear codes in the current channel conditions are $\rho_1 = 0, \rho_2 = 0$ and $\rho_3 = 0$ which is the same as the general encoding case $\rho = 0$. This is because the relay-destination channel is very strong and does not need any assistance from the source.

We show the performance of a 16-QAM constellation in Fig. 14 where $d_{12} = 1.5$ and $\alpha = 2$. The total rate transmitted from the source node to the destination node is $R = 3.5$. In this case, we used non-linear codes only at one of the least significant bits to provide the necessary gain and linear codes at the other three levels.

Remark 9: As mentioned earlier, to avoid rate loss, the source-relay codes need a non-uniform marginal distribution, which is not available via a (full-rank) linear code. In this section, we used DVB-S2 codewords in which a prescribed number of randomly-located binary symbols were converted to zero. A practical implementation of this scheme requires a pseudo-random number generator at the transmitter and receiver and the maintenance of synchrony between them.[5] An alternative approach is non-random assignment of zeros using a puncture design method [27]. Figures 12, 13, and 14 represent simulations where superposition codes were constructed with DVB-S2 codes together with random zero assignment; parallel experiments with puncturing design resulted in roughly similar performance, i.e., within 0.2 to 0.3dB of the experiments with random zero assignment.

VII. Discussion and Conclusion

Multilevel coding in the decode and forward relay channel is studied. A coded modulation technique is proposed where the correlation between the source signal and the relay signal

[5]If the decoder does not know the locations of these zeros, there will be a performance penalty of 1 to 1.5dB in performance.

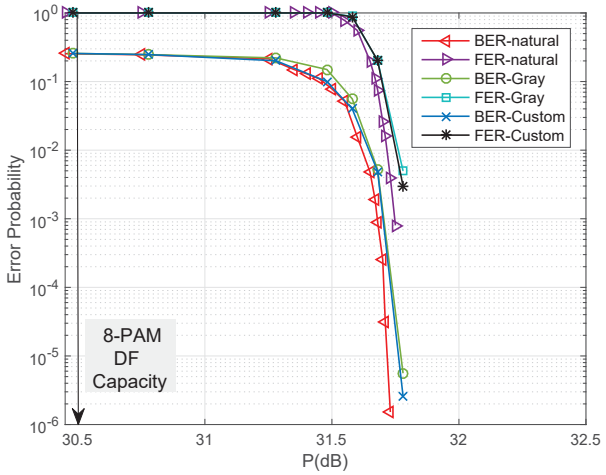

Fig. 13. Performance of Multilevel superposition for 8-PAM constellation with source-relay distance = 2.5

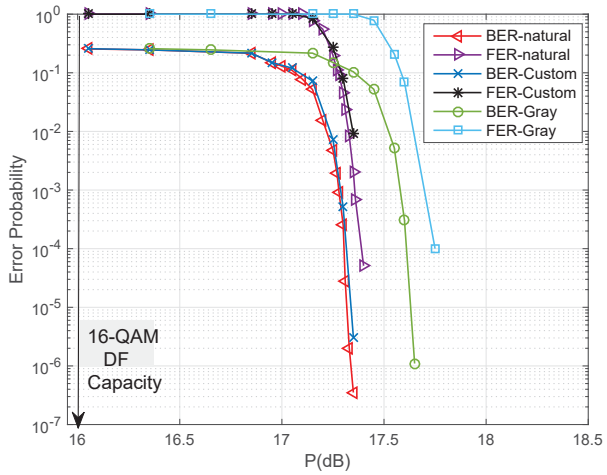

Fig. 14. Performance of Multilevel superposition for 16-QAM constellation with source-relay distance = 1.5

is controlled by the pairwise correlation between each level in the source and the corresponding level at the relay. Multistage decoding is studied and the necessary rates of each level for two different ways of multistage decoding are derived. A simple implementation of the proposed transmission using binary addition is presented. The labeling design is addressed and guidelines for it are presented. The error exponent of the proposed transmission is also studied, showing the loss in error exponent due to the proposed transmission is small. Numerical results show that the proposed multilevel coded modulation enjoys capacity approaching performance. From the implementation viewpoint, it is shown that a performance that is very close to the constellation constrained capacity is obtained by using standard point-to-point LDPC codes as component multi-level codes for the relay channel.

One of the main features of the present work is that it provides a systematic design process that is easily adapted to a variety of channel conditions (SNRs and rates). Furthermore, since the design of the coded modulation is reduced to the design of point-to-point binary codes, it enjoys a number of advantages including availability at a wide range of block lengths.

REFERENCES

[1] A. Khandani, "Two-way (true full-duplex) wireless," in *13th Canadian Workshop on Information Theory (CWIT)*, June 2013, pp. 33–38.

[2] A. Sabharwal, P. Schniter, D. Guo, D. Bliss, S. Rangarajan, and R. Wichman, "In-band full-duplex wireless: Challenges and opportunities," *IEEE J. Select. Areas Commun.*, vol. 32, no. 9, Sept. 2014.

[3] E. Ahmed, A. Eltawil, and A. Sabharwal, "Rate gain region and design tradeoffs for full-duplex wireless communications," *IEEE Trans. Wireless Commun.*, vol. 12, no. 7, pp. 3556–3565, July 2013.

[4] T. Riihonen, S. Werner, and R. Wichman, "Hybrid Full-Duplex/Half-Duplex relaying with transmit power adaptation," *IEEE Trans. Wireless Commun.*, vol. 10, no. 9, pp. 3074–3085, Sept. 2011.

[5] O. Agazzi, D. Messerschmitt, and D. Hodges, "Nonlinear echo cancellation of data signals," *IEEE Trans. Commun.*, vol. 30, no. 11, pp. 2421–2433, Nov. 1982.

[6] W. Afifi and M. Krunz, "Incorporating self-interference suppression for full-duplex operation in opportunistic spectrum access systems," *IEEE Trans. Wireless Commun.*, vol. 14, no. 4, pp. 2180–2191, Apr. 2015.

[7] T. Riihonen, S. Werner, and R. Wichman, "Mitigation of loopback self-interference in full-duplex MIMO relays," *IEEE Trans. Signal Processing*, vol. 59, no. 12, pp. 5983–5993, Dec. 2011.

[8] M. Duarte, "Full-duplex wireless: Design, implementation and characterization," Ph.D. dissertation, Rice University, 2012.

[9] S. Hong, J. Brand, J. I. Choi, M. Jain, J. Mehlman, S. Katti, and P. Levis, "Applications of self-interference cancellation in 5G and beyond," *IEEE Communications Magazine*, vol. 52, no. 2, pp. 114–121, 2014.

[10] D. Korpi, T. Riihonen, V. Syrjälä, L. Anttila, M. Valkama, and R. Wichman, "Full-duplex transceiver system calculations: Analysis of ADC and linearity challenges," *IEEE Trans. Wireless Commun.*, vol. 13, no. 7, pp. 3821–3836, 2014.

[11] A. Balatsoukas-Stimming, A. C. Austin, P. Belanovic, and A. Burg, "Baseband and RF hardware impairments in full-duplex wireless systems: experimental characterisation and suppression," *EURASIP Journal on Wireless Communications and Networking*, vol. 2015, no. 1, p. 1, 2015.

[12] T. Cover and A. Gamal, "Capacity theorems for the relay channel," *IEEE Trans. Inform. Theory*, vol. 25, no. 5, pp. 572–584, Sept. 1979.

[13] A. Chakrabarti, A. de Baynast, A. Sabharwal, and B. Aazhang, "Low density parity check codes for the relay channel," *IEEE J. Select. Areas Commun.*, vol. 25, no. 2, pp. 280–291, Feb. 2007.

[14] T. V. Nguyen, A. Nosratinia, and D. Divsalar, "Bilayer protograph codes for half-duplex relay channels," *IEEE Trans. Wireless Commun.*, vol. 12, no. 5, pp. 1969–1977, May 2013.

[15] P. Razaghi and W. Yu, "Bilayer low-density parity-check codes for decode-and-forward in relay channels," *IEEE Trans. Inform. Theory*, vol. 53, no. 10, pp. 3723–3739, Oct. 2007.

[16] N. Ferdinand, M. Nokleby, and B. Aazhang, "Low-density lattice codes for full-duplex relay channels," *IEEE Trans. Wireless Commun.*, vol. 14, no. 4, pp. 2309–2321, Apr. 2015.

[17] H. Imai and S. Hirakawa, "A new multilevel coding method using error-correcting codes," *IEEE Trans. Inform. Theory*, vol. 23, no. 3, pp. 371–377, 1977.

[18] U. Wachsmann, R. F. H. Fischer, and J. Huber, "Multilevel codes: theoretical concepts and practical design rules," *IEEE Trans. Inform. Theory*, vol. 45, no. 5, pp. 1361–1391, 1999.

[19] K. Ishii, K. Ishibashi, and H. Ochiai, "Multilevel coded cooperation for multiple sources," *IEEE Trans. Wireless Commun.*, vol. 10, no. 12, pp. 4258–4269, Dec. 2011.

[20] K. Ravindran, A. Thangaraj, and S. Bhashyam, "LDPC codes for network-coded bidirectional relaying with higher order modulation," *IEEE Trans. Commun.*, vol. 63, no. 6, pp. 1975–1987, June 2015.

[21] Z. Chen and H. Liu, "Spectrum-efficient coded modulation design for two-way relay channels," *IEEE J. Select. Areas Commun.*, vol. 32, no. 2, pp. 251–263, Feb. 2014.

[22] Z. Chen, B. Xia, Z. Hu, and H. Liu, "Design and analysis of multi-level physical-layer network coding for Gaussian two-way relay channels," *IEEE Trans. Commun.*, vol. 62, no. 6, pp. 1803–1817, June 2014.

[23] B. Hern and K. Narayanan, "Multilevel coding schemes for compute-and-forward with flexible decoding," *IEEE Trans. Inform. Theory*, vol. 59, no. 11, pp. 7613–7631, Nov. 2013.

[24] A. A. Abotabl and A. Nosratinia, "Broadcast coded modulation: Multi-level and bit-interleaved construction," *IEEE Trans. Commun.*, vol. 65, no. 3, pp. 969–980, Mar. 2017.

[25] A. Abotabl and A. Nosratinia, "Multilevel coding for the full-duplex relay channel," in *IEEE Global Communications Conference (GLOBECOM)*, Dec. 2015, pp. 1–6.

[26] ——, "Multi-level coding and multi-stage decoding in MAC, broadcast, and relay channel," in *IEEE International Symposium on Information Theory*, June 2014, pp. 96–100.

[27] M. Smolnikar, T. Javornik, M. Mohorcic, S. Papaharalabos, and P. T. Mathiopoulos, "Rate-compatible punctured DVB-S2 LDPC codes for DVB-SH applications," in *International Workshop on Satellite and Space Communications*, Sept. 2009, pp. 13–17.

[28] A. Ingber and M. Feder, "On the optimality of multilevel coding and multistage decoding," in *IEEE 25th Convention of Electrical and Electronics Engineers in Israel.*, Dec. 2008, pp. 731–735.

[29] N. Shende, O. Gurbuz, and E. Erkip, "Half-duplex or full-duplex relaying: A capacity analysis under self-interference," in *47th Annual Conference on Information Sciences and Systems (CISS)*, Mar. 2013, pp. 1–6.

[30] E. Ahmed and A. M. Eltawil, "All-digital self-interference cancellation technique for full-duplex systems," *IEEE Trans. Wireless Commun.*, vol. 14, no. 7, pp. 3519–3532, July 2015.

[31] K. Alexandris, A. Balatsoukas-Stimming, and A. Burg, "Measurement-based characterization of residual self-interference on a full-duplex MIMO testbed," in *IEEE 8th Sensor Array and Multichannel Signal Processing Workshop (SAM)*, June 2014, pp. 329–332.

[32] N. H. Mahmood, I. S. Ansari, G. Berardinelli, P. Mogensen, and K. A. Qaraqe, "Analysing self interference cancellation in full duplex radios," in *IEEE Wireless Communications and Networking Conference*, Apr. 2016, pp. 1–6.

[33] A. E. Gamal and Y. Kim, *Network Information Theory*. Cambridge University Press, 2012.

[34] A. Ingber and M. Feder, "Capacity and error exponent analysis of multilevel coding with multistage decoding," in *IEEE International Symposium on Information Theory*, June 2009, pp. 1799–1803.

[35] A. Bennatan, D. Burshtein, G. Caire, and S. Shamai, "Superposition coding for side-information channels," *IEEE Trans. Inform. Theory*, vol. 52, no. 5, pp. 1872–1889, May 2006.

[36] Q. Li and C. Georghiades, "On the error exponent of the wideband relay channel," in *Signal Processing Conference, 14th European*, Sept. 2006, pp. 1–5.

[37] G. Bradford and J. Laneman, "Error exponents for block markov superposition encoding with varying decoding latency," in *IEEE Information Theory Workshop ITW*, Sept. 2012, pp. 237–241.

[38] V. Tan, "On the reliability function of the discrete memoryless relay channel," *IEEE Trans. Inform. Theory*, vol. 61, no. 4, pp. 1550–1573, Apr. 2015.

[39] A. Ingber and M. Feder, "Finite blocklength coding for channels with side information at the receiver," in *IEEE 26th Convention of Electrical and Electronics Engineers in Israel (IEEEI)*, Nov. 2010, pp. 000 798–000 802.

[40] G. Kramer, M. Gastpar, and P. Gupta, "Cooperative strategies and capacity theorems for relay networks," *IEEE Trans. Inform. Theory*, vol. 51, no. 9, pp. 3037–3063, Sept. 2005.

[41] A. Chakrabarti, A. Sabharwal, and B. Aazhang, "Sensitivity of achievable rates for half-duplex relay channel," in *IEEE 6th Workshop on Signal Processing Advances in Wireless Communications*, June 2005, pp. 970–974.

Ahmed Attia Abotabl (S'15, M'17) received the B.S. degree (Hons.) from Alexandria University, Egypt, M.Sc. degree from Nile University, Egypt and the Ph.D. degree from the University of Texas at Dallas, Richardson, TX, USA, all in electrical engineering. He is currently a Senior Engineer at Samsung SOC US R&D center, San Diego, CA, where he is involved in algorithm development for 5G wireless modems. His research interests include information theory, coding theory and their applications in physical layer security, and machine learning. He received the UTD Electrical Engineering Industrial Advisory Board Award in 2016, the Louis-Beecherl Jr. Award in 2015, and the Erik Jonsson Graduate Fellowship in 2012 from the University of Texas at Dallas.

Aria Nosratinia (S'87-M'97-SM'04-F'10) is Erik Jonsson Distinguished Professor and associate head of the Electrical Engineering Department at the University of Texas at Dallas. He received his Ph.D. in Electrical and Computer Engineering from the University of Illinois at Urbana-Champaign in 1996. He has held visiting appointments at Princeton University, Rice University, and UCLA. His interests lie in the broad area of information theory and signal processing, with applications in wireless communications. He was the secretary for the IEEE Information Theory Society in 2010-2011 and was the treasurer for ISIT 2010 in Austin, Texas. He has served as editor for the IEEE Transactions on Information Theory, IEEE Transactions on Wireless Communications, IEEE Signal Processing Letters, IEEE Transactions on Image Processing, and IEEE Wireless Communications (Magazine). He has been the recipient of the National Science Foundation career award, and is a fellow of IEEE. He was named a Thomson Reuters highly cited researcher.